# Exploiting Chaotic Dynamics for Detecting Parametric Variations in Aeroelastic Systems

Bogdan I. Epureanu*
*University of Michigan, Ann Arbor, Michigan 48109*
and
Liaosha S. Tang[†] and Michael P. Païdoussis[‡]
*McGill University, Montreal, Quebec H3A 2K6, Canada*

A panel forced by buffeting aerodynamic loads and undergoing limit-cycle oscillations and chaos is investigated. The interaction of dynamic and static instabilities is shown to lead to very complex dynamics, which includes static deformations, limit-cycle oscillations, and chaos. The sensitivity of the chaotic behavior to parametric changes is shown to be an effective tool in detecting structural changes such as variations in the stiffness of the mounting point of the upstream end of the panel. A finite difference method is used to simulate the dynamics of the aeroelastic system, and coherent structures of the panel dynamics are identified using proper orthogonal decomposition. The sensitivity of the dynamics of the coherent structures to parametric changes is discussed.

## Introduction

LINEAR vibration analysis is a relatively mature field of mechanical engineering, although there are several areas of this field where investigations are still necessary, such as mid-frequency analysis. In contrast, the field of nonlinear and chaotic vibrations presents many challenges and has recently recaptured the interest of researchers in academia and industry especially because many engineering systems, previously approximated as being linear, are in fact nonlinear. In structural dynamics, for example, nonlinearity is often observed, and it is due to friction, the presence of rivets, bolts, free play, and other factors. Nonlinear phenomena are widespread and very important because their presence can dramatically change the predictions made by linear theories. For example, nonlinearities are the cause of parametric resonances and limit-cycle oscillations, which are incompletely modeled by linear approaches. Moreover, the recent remarkable advances in the understanding of nonlinear and chaotic phenomena provide the means to exploit their features for detecting parametric changes in various systems, that is, for structural health monitoring.

The area of health monitoring and damage detection has undergone a rapid development recently, and new methods and techniques continue to be proposed.[1] Health monitoring refers to the use of nondestructive sensing and analysis of system characteristics for the purpose of detecting structural changes which may indicate damage.[2] Health monitoring is often approached as a system identification problem,[3] where changes in the parameters of an identified model are monitored.[4−6] A large portion of the work in this area has been focused on least-squares identification methods applied to linear models,[7−10] resonant frequencies,[11] mode shapes,[12] and subspace identification methods.[13,14] Most system identification procedures used for structural health monitoring are based on off-line approaches,[15] although recently online damage detection methods

have been proposed as well.[16,17] Also, the Yorke–Kaplan conjecture from complex system theory has been used at the U.S. Naval Research Laboratory NRL for the pioneering study of linear systems with chaotic excitation (see Refs. 18 and 19). Both numerical[20] and experimental[21] investigations of linear structures have been performed. However, most of the current studies are based on linear theories and linear structures. In contrast, this paper is focused on chaotic dynamics and has the potential advantage of an increased accuracy in detecting damage and monitoring structural health. The increased accuracy obtained by exploiting the sensitivity of nonlinear and chaotic systems to parametric variations is shown herein to be 4–5 orders of magnitude higher than the sensitivity of linear analyses.

In addition to these particularities of chaotic dynamics, the feature monitored to detect structural changes is the level of coherence in the dynamics of the system. The approach used for identifying these coherent structures is proper orthogonal decomposition (POD).[22−24] This approach requires measurements of the dynamics of the system of interest over a time interval. A model for the spatial coherence of the dynamics is constructed based on these measurements. For linear systems, the models obtained using POD are similar to models obtained by modal analyses. However, distinct from linear modal analyses, POD may be used for nonlinear systems. Holmes et al.[25] and Sirovich[26] also used POD in the context of turbulent flows as a technique that allows for the identification of naturally forming coherent structures from numerical simulations or experiments. These coherent structures contain most of the energy and are the most important components of the dynamics.[27−29]

The physical system investigated herein is a panel forced by buffeting aerodynamic loads. Such panels in the supersonic flow regime have been studied extensively by Dowell and Voss[30] and Dowell.[31−35] They observed that the interaction of dynamic (flutter) and static (buckling) instabilities leads to very complex dynamics, which includes static deformations, limit-cycle oscillations, and chaos. Most of the previous studies of the dynamics of panels under buffeting aerodynamic load are based on the Galerkin method for numerical simulations. Distinct from those methods, a finite difference method is used herein, and POD[23−25,36] is used to detect parametric changes in the aeroelastic system. The numerical method based on POD requires a small number of degrees of freedom for capturing accurately the dynamics of the panel while maintaining its sensitivity to parametric changes. This sensitivity is shown to be an effective tool in detecting structural modifications, such as variations in the stiffness of the mounting point of the upstream end of the panel.

*Assistant Professor, Department of Mechanical Engineering, 3138 G. G. Brown Building; epureanu@umich.edu. Member AIAA.

[†]Graduate Student and Research Assistant, Department of Mechanical Engineering; liaosha@freedom. mecheng.mcgill,ca.

[‡]Thomas Workman Emeritus Professor, Department of Mechanical Engineering; mary.fiorilli@mcgill.ca.
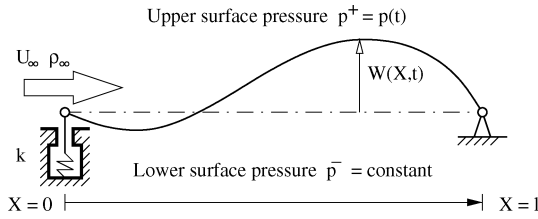
**Fig. 1 Two-dimensional buffeting panel.**

## Modeling

The aeroelastic model used is shown in Fig. 1 and includes structural nonlinearities, whereas the aerodynamics is considered quasi static and linear. The flow is modeled using piston theory, and the panel is modeled using nonlinear plate theory. The coupling of the aerodynamic and structural models is done by a balancing of the pressure differentials across the panel with the elastic and inertial forces in the panel.

### Flow Model

The piston theory is a simplified method developed by Lighthill[37] and is a good approximation of the unsteady flow forces for large Mach numbers and low frequencies. For such cases, Lighthill showed that the flow may be modeled as a series of fluid slabs, contained between vertical planes, perpendicular to the panel. Each of the slabs is approximated by a walled container, full of fluid and bounded by the surface of the panel at its lower end. Then, the panel acts like a piston moving the fluid and generates compression and expansion waves inside the container. The unsteady component of the pressure created by the presence of the flow on the upper surface of the panel due to panel motion may be expressed as

$$p(t) = -(h/l)\left(\rho_\infty U_\infty^2 / M\right)W' - \left(\sqrt{Dh}/l^2\right)\left(\rho_\infty U_\infty / M\sqrt{\rho}\right)\dot{W}$$
(1)

where $\rho_\infty$ and $U_\infty$ are the upstream far field density and velocity of the flow, $M$ is the local Mach number, $W$ is the transverse deformation of the panel, and $W'$ and $\dot{W}$ are the spatial and time derivatives of $W$, respectively. The minus sign is due to the sign convention used for the full aeroelastic model and indicates that this pressure acts downward, while the panel deflection is considered positive upward.

### Structural Model

The panel shown in Fig. 1 is considered to be a homogeneous, isotropic, and two-dimensional plate, with pinned–pinned endpoints. A supersonic flow is forcing the panel along its upper surface. The lower surface of the panel is considered isolated from the flow and at a constant pressure. In addition, a longitudinal preload acts on the panel at its pinned ends and provides a compression load in the panel. The flow is considered two dimensional (along $X$ and $W$), and thus, the plate may be assumed one dimensional (along its chord $X$), while its span is considered infinite.

The von Kármán nonlinear strain–displacement relation for large deflections of the panel (see Ref. 34) may be used to obtain the following governing equation of the panel dynamics:

$$W'''' - \frac{Eh^3}{2D}\left[\int_0^1 W'^2(\xi)\,d\xi\right]W'' - \frac{Eh\eta l^2}{D}W'' + \ddot{W} + \frac{l^4}{Dh}\Delta p = 0$$
(2)

where $\Delta p$ is the steady and unsteady pressure difference between upper and lower surfaces, $\Delta p = p^+ - p^-$; $h$ and $l$ are the thickness and the length of the panel, respectively, with $l \gg h$; $E$, $\nu$, and $\rho$ are Young's modulus, the Poisson ratio, and the mass density of the panel material, respectively; $D$ is a coefficient characterizing the bending stiffness of the panel, $D = Eh^3/12(1 - \nu^2)$. The structural nonlinearity is due to the quadratic integral term in Eq. (2).

For the case of an infinitely stiff spring at the upstream end of the panel, the boundary conditions corresponding to the pinned–pinned

panel may be expressed as

$$W(X = 0, t) = 0, \qquad W''(X = 0, t) = 0$$

$$W(X = l, t) = 0, \qquad W''(X = l, t) = 0$$

However, the presence of the spring allows the upstream end to move, and a shear force is created thereby. The boundary conditions at the upstream end may be expressed as

$$W''(X = 0, t) = 0$$

$$kW(X = 0, t) - DW'''(X = 0, t) = 0$$

where $k$ is the stiffness of the upstream panel attachment point/spring. The nondimensional expression used for this stiffness is $R$ defined as $R = D/(kl^3)$. Thus, for example, a rigid attachment point is characterized by $R = 0$.

### Aeroelastic Model

The aeroelastic model is obtained by inserting the expression for the pressure differential across the plate given by Eq. (1) into Eq. (2). The aeroelastic equation thus obtained is then nondimensionalized by considering the variables $x$, $w$, and $\tau$, defined as $x = X/l$, $w = W/h$, and $\tau = t/\sqrt{(\rho h l^4/D)}$. The aeroelastic model in nondimensional form may be expressed as

$$w'''' + \ddot{w} - \frac{Eh\eta l^2}{D}w'' - \frac{Eh^3}{2D}\left[\int_0^1 w'^2(\xi)\,d\xi\right]w''$$

$$+ \frac{\rho_\infty U_\infty^2 l^3}{MD}w' + \frac{\rho_\infty U_\infty l^2}{M\sqrt{\rho h D}}\dot{w} + \frac{l^4}{Dh}\Delta p_s = 0$$
(3)

where $\dot{w} = \partial w/\partial\tau$, $w' = \partial w/\partial x$, and $\Delta p_s$ is the static/steady pressure differential across the plate, that is, the pressure difference at zero flow velocity, $U_\infty = 0$.

Nondimensional coefficients are obtained from Eq. (3) as follows. The flow velocity is characterized by $\lambda$, where $\lambda = (\rho_\infty U_\infty^2 l^3)/(MD)$. The in-plane preload of the panel is proportional to $R_x$, which is given by $R_x = Eh\eta l^2/D$. The static pressure difference across the panel is characterized by $P$, where $P = -(l^4 \Delta p_s)/(Dh)$. The panel material is characterized by $G = (Eh^3)/(2D) = 6(1 - \nu^2)$. The mass ratio is given by $\mu = (\rho_\infty l)/(\rho h)$. These parameters may be used in Eq. (3) to obtain

$$\ddot{w} + \sqrt{\frac{\mu\lambda}{M}}\dot{w} + w'''' - R_x w'' - G\left[\int_0^1 w'^2(\xi)\,d\xi\right]w'' + \lambda w' = P$$
(4)

The aeroelastic system governed by Eq. (4) is a convenient and simplified version of a more realistic system, and thus, its parameters have estimated values. Nevertheless, the results (and assumptions made) are useful to demonstrate the key ideas and techniques proposed. Also, this aeroelastic system shows that the methods proposed could be used to study other, more realistic, systems.

## Numerical Discretization

Standard central finite difference schemes of second-order accuracy are used to discretize all of the spatial derivatives. First, the panel is discretized in $s$ sections. Also, ghost nodes are used at each end of the computational domain, so that there are a total of $s + 3$ discretization points. The displacements at each of the discretization points are grouped in a vector $w$ so that, at a nondimensional time instant $\tau_k$, the shape of the panel is defined by a vector $w^k = [w_{-1}^k, w_0^k, \ldots, w_{s+1}^k]^T$. The discretized spatial derivatives are considered linear operators applied to the vector $w^k$. The first through fourth spatial derivative operators are $(s + 3) \times (s + 3)$ matrices, denoted by $D_1$–$D_4$.

The boundary conditions for Eq. (4) are linear operators acting on the vector $w^k$ also. The implementation of these boundary conditions is obtained by adequately changing the first and last two rows of the matrices $D_i$. The boundary conditions apply to $w$ directly and can

be referred to in a compact form as a zero linear operator $D_0$, which is a $(s+3) \times (s+3)$ identity matrix with the first and last two rows modified to incorporate the boundary conditions.

The discretized form of Eq. (4) incorporates the boundary conditions and is expressed as

$$[c_4 D_4 + c_3 D_3 + c_2 D_2 + c_1 D_1 + c_0 D_0]w$$

$$+ c_5(w^T T w)D_2 w + c_6 \ddot{w} + c_7 \dot{w} = q \qquad (5)$$

where $c_0$–$c_7$ are constant coefficients given by $c_4 = 1$, $c_3 = 0$, $c_2 = -R_x$, $c_1 = \lambda$, $c_0 = 0$, $c_5 = -G$, $c_6 = 1$, and $c_7 = \sqrt{(\mu\lambda/M)}$. The term $w^T T w$ is a discrete representation of the integral term in Eq. (4), with $T$ being an $(s+3) \times (s+3)$ constant matrix. The right-hand side $q$ incorporates the discretization of the distributed static load due to the static pressure difference across the plate $\Delta p_s$. Equation (5) may be expressed in state-space matrix form as

$$\begin{bmatrix} I & 0 \\ 0 & A \end{bmatrix} \begin{bmatrix} \dot{w} \\ \dot{v} \end{bmatrix} + \begin{bmatrix} 0 & -I \\ M & B \end{bmatrix} \begin{bmatrix} w \\ v \end{bmatrix} = \begin{bmatrix} 0 \\ q \end{bmatrix} \qquad (6)$$

where $v = \dot{w}$, $A = c_6 I$, and $B = c_7 I$, with $c_6 I$ and $c_7 I$ being identity matrices multiplied by the constant coefficients $c_6$ and $c_7$ and having the first and last two rows replaced by boundary conditions. The matrix $M$ is given by $M = c_4 D_4 + c_3 D_3 + (c_2 + c_5 w^T T w)D_2 + c_1 D_1 + c_0 D_0$, with its first and last two rows also including boundary conditions.

## Coherent Structures

The discretized model presented in the preceeding section is accurate and requires a moderate computational effort to predict the dynamics of the aeroelastic system. The results obtained can be used for identifying coherent structures. One of the techniques used for extracting these coherent structures present in the dynamics of the system is POD.[23,24,26−29] To apply the POD method, the finite difference method is first used to obtain snapshots of the state of the panel at a series of time instants. These snapshots are organized as column vectors in a matrix $R$ so that $R = [w^{k_1}, w^{k_2}, \ldots, w^{k_m}]$, where $k_i$ are $m$ time instants where the snapshots are collected. A two-point correlation matrix $C$ is then formed, $C = R^T R$. The matrix $C$ is a real $m \times m$ symmetric matrix, which is positive or semipositive definite and has a set of real eigenvalue–eigenvector pairs. The eigenvalues and eigenvectors of the matrix $C$ are denoted by $\lambda_1$, $\lambda_2$, $\ldots$, $\lambda_m$ and $e_1$, $e_2$, $\ldots$, $e_m$. They are organized in decreasing order, that is, $\lambda_i \geq \lambda_{i+1}$. The largest eigenvalues correspond to dominant structures in the dynamics of the panel. Thus, the first $n$ eigenvectors represent dominant structures and are selected, with $n \ll m$. Next, the shapes of the $n$ dominant structures are obtained as $b_i = R e_i$, $i = 1, 2, \ldots, n$.

The shape of the panel may be approximated as a linear combination of dominant structures $b_i$. The vectors $b_i$ are grouped as columns of an $N \times n$ matrix $P$, that is, $P = [b_1, b_2, \ldots, b_n]$. The shape $w$ and velocity $v$ of the panel points are approximated as

$$w = P\tilde{w}, \qquad v = P\tilde{v} \qquad (7)$$

where $\tilde{w}$ and $\tilde{v}$ are $n$-dimensional vectors. Substituting Eq. (7) into Eq. (6) and left multiplying the result by

$$\begin{bmatrix} P^T & 0 \\ 0 & P^T \end{bmatrix}$$

one obtains a model for the dynamics of the coherent structures as

$$\begin{bmatrix} P^T P & 0 \\ 0 & P^T P \end{bmatrix} \begin{bmatrix} \dot{\tilde{w}} \\ \dot{\tilde{v}} \end{bmatrix} + \begin{bmatrix} 0 & -P^T P \\ P^T A^{-1} M P & P^T A^{-1} B P \end{bmatrix} \begin{bmatrix} \tilde{w} \\ \tilde{v} \end{bmatrix}$$

$$= \begin{bmatrix} 0 \\ P^T A^{-1} q \end{bmatrix} \qquad (8)$$

The full model is first integrated in time, and time series are collected. Then, snapshots of the shape of the panel are selected and

used to obtain a model for the dynamics of the dominant structures. The convergence of the full-order finite difference method with respect to the number of spatial discretization points has been carefully tested, and $s = 100$ has been found to be a satisfactory choice. For the same considerations of convergence, the time step used to integrate Eq. (6) in time has been set to $\tau = 0.01$. The time integration has been carried out using the Gear method and the solver provided by the International Mathematics and Statistics Libraries (IMSL).

## Numerical Results

Chaotic dynamics is typically more sensitive to parametric variations than other types of behavior. For example, stable limit-cycle oscillations of the panel forced by aerodynamic loads are less influenced by the changes in the rigidity of the upstream mounting point. Figure 2 shows that the limit cycles of the aeroelastic system are virtually identical for two very different rigidities, $R = 0$ and $R = 2 \times 10^{-5}$. The parameters of the aeroelastic system undergoing limit-cycle oscillations are $R_x = -2\pi^2$, $\lambda = 350$, $P = 0$, $\nu = 0.3$, and $\mu/M = 0.01$.

To investigate the sensitivity of the chaotic dynamics to parametric changes, a set of parameters of the aeroelastic system have been chosen based on a bifurcation diagram of the dynamics, as shown in Fig. 3. A chaotic regime has been selected by setting the parameters to $R_x = -4\pi^2$, $\lambda = 150$, $P = 5$, $\nu = 0.252$, and $\mu/M = 0.01$.
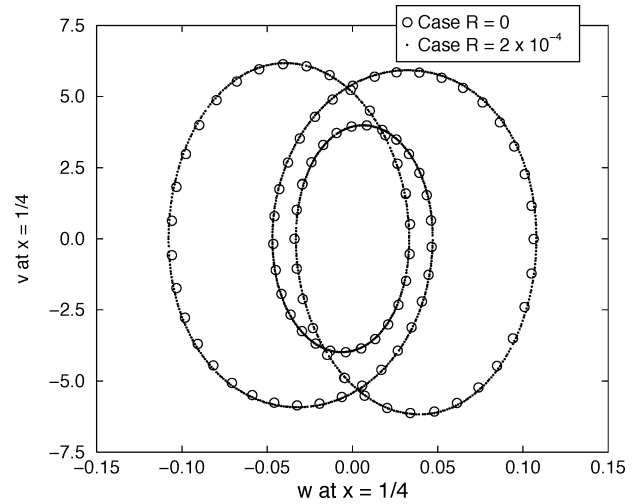


Fig. 2   State-space plot of quarter point displacement for two distinct parameters $R$ corresponding to two distinct stiffnesses $k$ of the upstream endspring and a panel exhibiting limit-cycle oscillations.
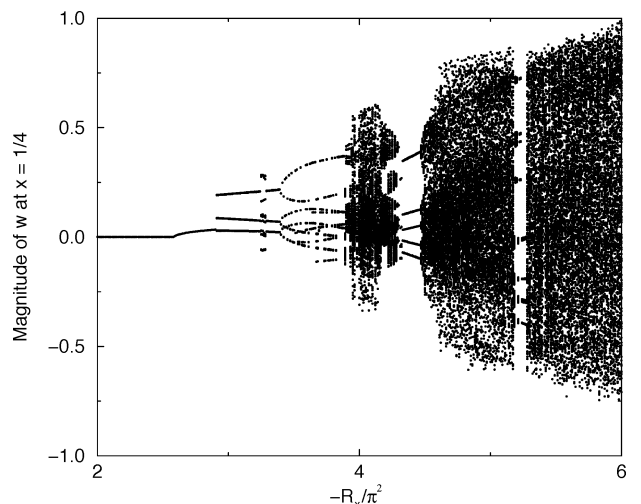


Fig. 3   Bifurcation diagram of the magnitude of the quarter point displacement for varying $R_x$.

These parameters have been chosen to ensure the presence of chaotic dynamics. Indeed the significant advantages of the proposed analysis are accompanied by a limitation, that is, the requirement that a chaotic oscillation be present. Nevertheless, this limitation may be overcome when a chaotic excitation may be provided to the system, for example, such excitation has been used successfully in other research.[19] Also, such dynamic behavior has been observed in many applications in industries such as aerospace, nuclear, telecommunications, and sensors (wings,[34,38–41] panels forced by flow-induced loads,[42–49] rotors,[50] pipes,[51–53] heat exchangers,[51,54–56] microsystems[57,58] such as microplates). Also, other studies of similar aeroelastic systems provide additional details in regard to the parameter range where chaotic dynamics occurs.[35,48,49]

Time series obtained for four distinct nondimensional rigidities are shown in Fig. 4: case a, $R = 0$; case b, $R = 1.739 \times 10^{-8}$; case c, $R = 2 \times 10^{-8}$; and case d, $R = 2 \times 10^{-7}$. For simplicity, only the displacement of the quarter point of the panel is shown, that is, $w$ at $x = \frac{1}{4}$. A clear distinction between cases a, c, and d can be observed. This distinction reflects the large differences in the rigidity of the upstream mounting point (which varies from zero to order $10^{-8}$, and then to order $10^{-7}$). A much finer distinction is observed between cases b and c, which correspond to stiffnesses differing by 15%. All four cases exhibit chaotic oscillations and are characterized by maximal Lyapunov exponents larger than 2.

The time series shown in Fig. 4 indicate that a simple observation of one point of the panel may reveal large parametric changes. For example, a qualitative difference may be observed between cases a, c, and d. However, small parametric changes may be more difficult to detect, as shown by the similarity between the time series for cases b and c. A more elaborate analysis is necessary to decompose the dynamics of the plate in components corresponding to coherent structures (or dominant modes) present in the dynamics. Moreover, several invariants of the dynamics, such as the fractal dimension of their attractors, are sensitive to large parametric variations and relatively insensitive to small variations. For example, Fig. 5 shows the fractal dimensions of the attractors of the dynamics for cases a–d using an embedding dimension of 12. The details about embedding dimensions and the calculation of fractal dimensions are omitted here for the sake of brevity, but they are provided in the literature.[59–63] The correlation (fractal) dimension $C(\epsilon)$ is plotted vs the box dimension $\epsilon$ in a log–log plot in Fig. 5 and shows a multifractal structure, with dimensions ranging approximately from 2.5 to 4.5. There is a clear distinction between cases a, b, and d, which correspond to large parametric variations. However, there is a small difference between cases b and c, where the parametric variation
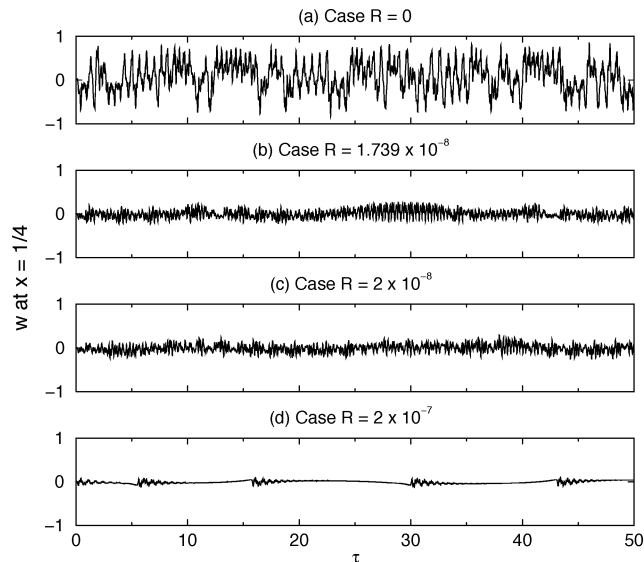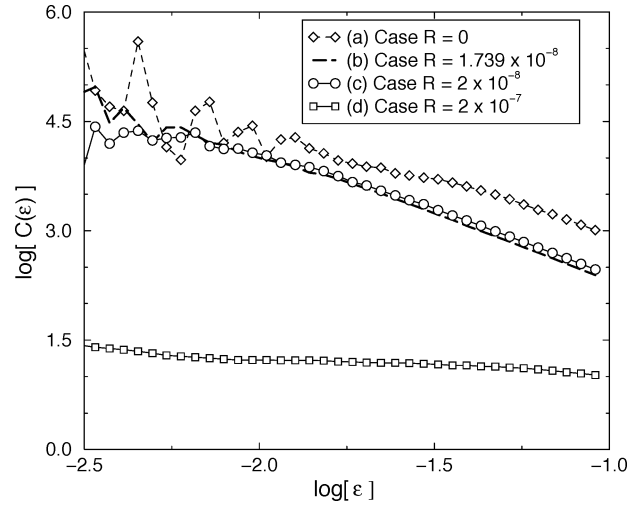


**Fig. 5    Fractal dimensions of embedded attractors for cases a–d using 12 embedded coordinates.**

is small. Nevertheless, a more detailed analysis of the attractor is capable of revealing small parametric changes. For example, the first-order inertial moment of the set of points representing the attractor in an embedded space with 6 and 12 dimensions shows a relative change of 25% in the largest inertial moment between cases b and c. This difference is substantial and robust to random noise. To test its robustness, we introduced white noise in the time series analyzed. The noise has has been considered to have a magnitude of 5% of the signal. The resulting change in the estimated largest inertial moment has been of less than 1%, which is much less than the change of 25% due to parametric variations.

The maximal Lyapunov exponents computed for all cases discussed are larger than 2, which is a result confirmed by the apparent lack of periodicity in Fig. 4. The fractal dimensions (shown in Fig. 5) and the maximal Lyapunov exponents are discussed to provide a means to compare the current approach to other methods based on nonlinear techniques presented in the literature.[18,19] The proposed method is not based on Lyapunov exponents or fractal dimensions for damage detection because of the difficulties regarding the practicality of experimental data collection required by such approaches. Moreover, the technique proposed shows a much larger sensitivity to parametric variations than the method based on Lyapunov exponents or fractal dimensions. Additionally, the geometric shape of the sampled attractor (in a Poincaré section) is much easier to obtain. For example, a sampling rate of about 100 samples per nondimensional period of the linearized aeroelastic system provides sufficient data for the proposed method in just a few (50–100) periods. Thus, for a system with a linearized natural frequency of about 100 Hz, just a few seconds are sufficient for collecting the necessary data.

The POD method is used, and a correlation matrix is obtained based on 100 snapshots collected over the time interval from $\tau = 0$ to $\tau = 50$. The eigenvalues $\lambda_i$ of this matrix are shown in Fig. 6. Similar snapshots are collected for each value of the upstream endpoint rigidity. The rapid decrease in the magnitude of the eigenvalues $\lambda_i$ indicates that a strong spatial correlation exists between the dynamics of various points on the panel. The spatial coherence is consistent with the temporal chaotic behavior observed in Fig. 4 because the dynamics of each coherent structure is chaotic in time. The six dominant POD eigenfunctions are shown in Fig. 7. Note that the shape of the dominant structures vary with the parameter $R$. However, the variation of the dominant modes is small even for large variations in the value of $R$.

The dynamics of each of the dominant coherent structures is chaotic, as shown in Fig. 8. However, qualitative differences may be observed between the four cases. Large differences are observed, especially for the first dominant coherent structure even for small parametric variations. To detect these changes, we computed Poincaré sections of the strange attractors of the dynamics of the quarter
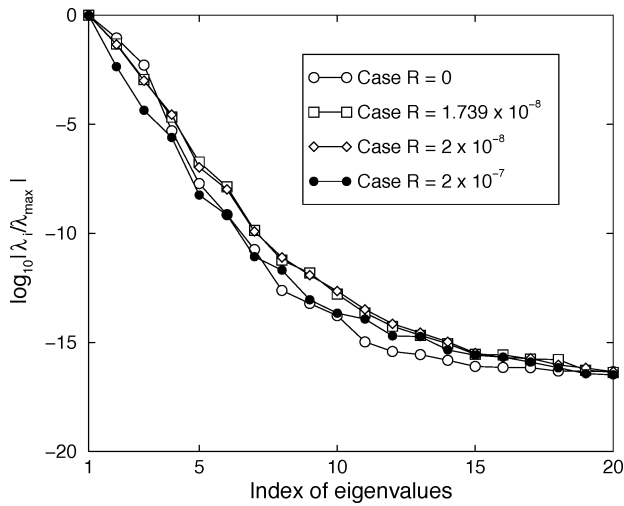


**Fig. 4    Time series of the quarter point displacement for four distinct parameters $R$ corresponding to four distinct stiffnesses $k$ of the upstream endspring.**

**Fig. 6  Eigenvalues of the correlation matrix for four distinct parameters $R$ corresponding to four distinct stiffnesses $k$ of the upstream end spring.**
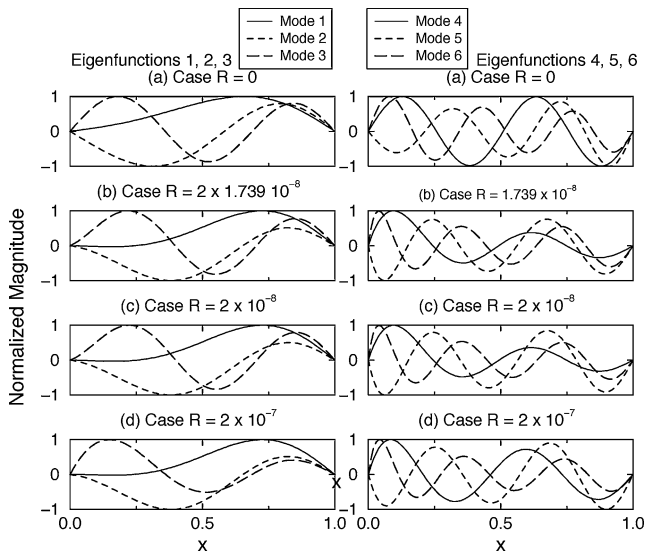


**Fig. 7  Dominant coherent structures for four distinct parameters $R$ corresponding to four distinct stiffnesses $k$ of the upstream endspring.**
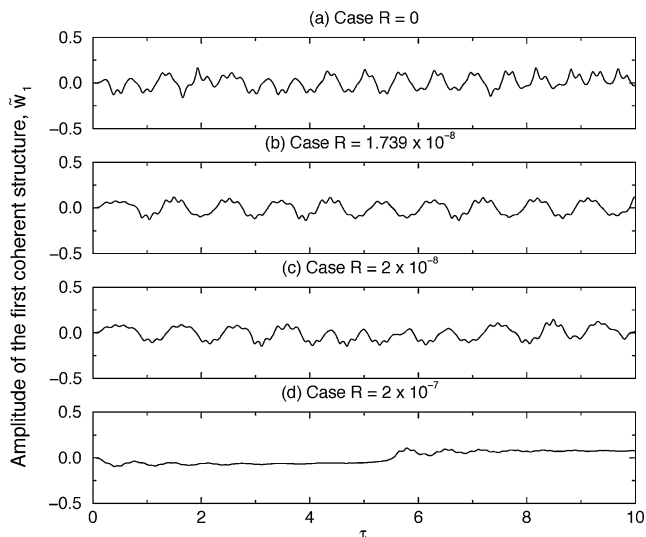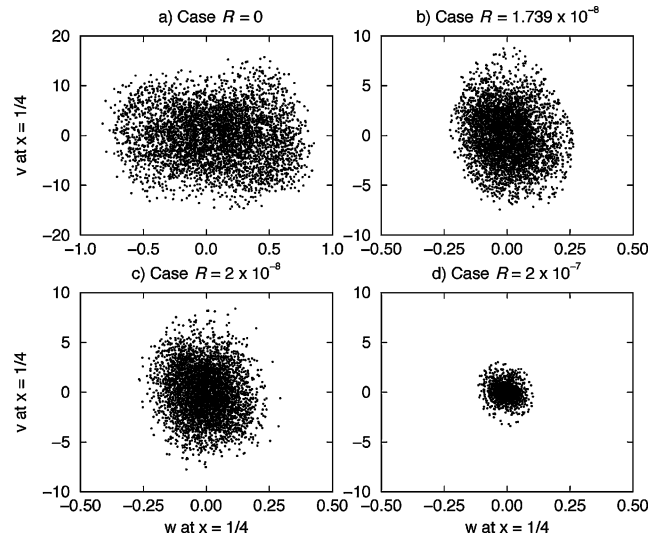


**Fig. 8  Time series of the first most dominant coherent structure for $R = 0$, that is, a rigid upstream spring, $R = 1.739 \times 10^{-8}$, $R = 2 \times 10^{-8}$, and $R = 2 \times 10^{-7}$.**



**Fig. 9  Poincaré plot of the first coherent structure for four distinct parameters $R$ corresponding to four distinct stiffnesses $k$ of the upstream endspring.**

point and each of the first six dominant coherent structures. These Poincaré sections were obtained by sampling in time at a frequency that was a priori chosen. For autonomous systems (such as the aeroelastic system discussed herein), the sampling interval for sections defined in time is problem dependent, and no definite choice is universal for all systems, although the sampling rate is somewhat related to the (order of magnitude of the) natural frequency of the system. A more usual choice would have been "every time the velocity of the $\frac{1}{8}$ point (or some other point but not the $\frac{1}{4}$ point) changes sign."[62] Nevertheless, the sections defined in time can also convey ideas about the behavior of the vector field. In the present investigation, the main period of the oscillation just before chaos has been computed, and based on that, the Poincaré sections were obtained by sampling in time at every 0.01 nondimensional time unit. Figure 9 shows the Poincaré section obtained for the quarter point. Similar to the observation of the time series shown in Fig. 4, the Poincaré sections reveal large parametric changes. (Note the scales of the vertical axes.) However, small parametric changes are not as easily observed. In contrast, the dynamics of the coherent structures provides much more detail. Figure 10 shows a clear distinction between the four cases. Observing these attractors, one may detect changes of as low as 15% in the stiffness of the upstream endspring. The first dominant coherent structure reveals these differences most clearly. Nevertheless, the dynamics of the other five (of the total of six) dominant coherent structures (not shown here for the sake of brevity) reveals the parametric changes also (but with less sensitivity).

The relative distribution of points in the Poincaré sections shown in Fig. 10 may be investigated and quantified using various techniques developed within the pattern recognition community[64,65] to detect changes in their geometric appearance. One of the simplest methods is based on histograms. Figure 11 shows the histogram obtained for cases b and c, where $R = 1.739 \times 10^{-8}$ and $R = 2 \times 10^{-8}$. A quantitative difference may be observed, especially around the maxima at $\tilde{w}_1 = \pm 0.075$. An even more dramatic difference is observed between cases a and d, where $R = 0$ and $R = 2 \times 10^{-7}$ (Fig. 12). More detailed analyses may be performed to quantify the differences in the shape and distribution of points of the attractors shown in Fig. 10. Nevertheless, the key aspect is that decomposing the dynamics of the aeroelastic panel along a basis of the vector space spanned by the dominant structures of the dynamics and employing Poincaré sections of the strange attractors for each coherent structure is a valid and powerful method for detecting parametric changes.

The effectiveness of the proposed technique may be estimated by comparing it to a standard linear analysis where stiffness loss in the
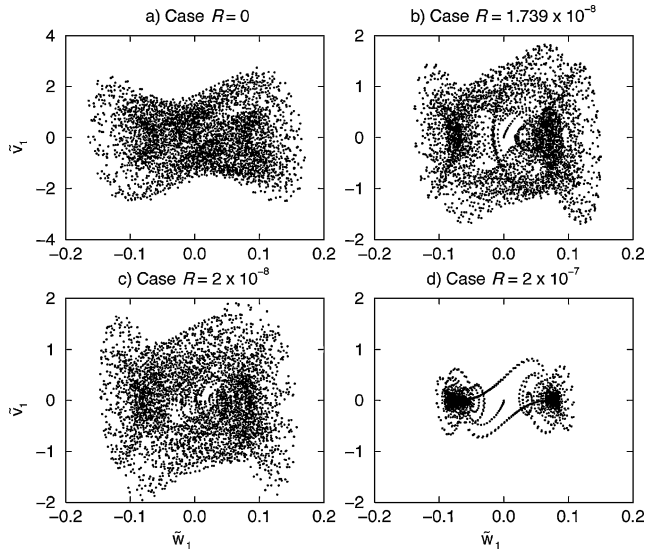
**Fig. 10  Poincaré plot of the quarter point displacement for four distinct parameters $R$ corresponding to four distinct stiffnesses $k$ of the upstream endspring.**
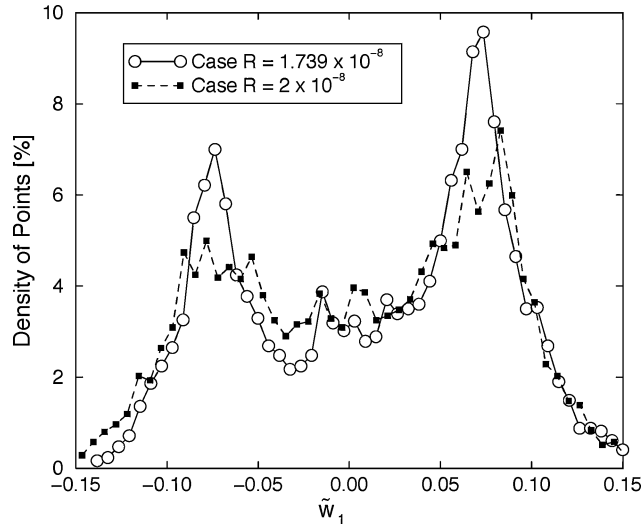


**Fig. 11  Histogram of the point distribution in the Poincaré plot for the first dominant mode for cases b and c.**
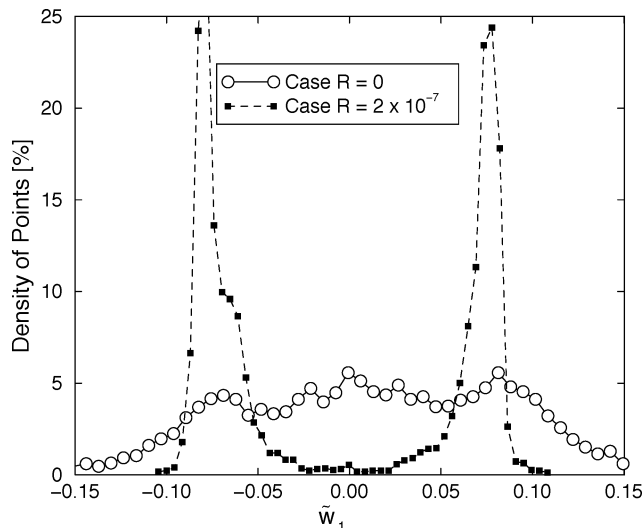


**Fig. 12  Histogram of the point distribution in the Poincaré plot for the first dominant mode for cases a and d.**

structure is monitored. A linear model may be obtained by setting the parameter $G$ in Eq. (4) to zero, that is, linearizing the model. Next, the modes and frequencies of vibration of the linearized system may be obtained. The frequencies of vibration have been determined for various stiffnesses of the upstream spring corresponding to $R$ values from zero to $10^{-5}$. Despite the large change in the parameter $R$ (an interval 100 times larger than the changes studied by nonlinear means), the variation of the first three (linear) modes and frequencies has been very small, of a magnitude less than 0.05%. In contrast, the monitored features obtained by the nonlinear analysis are much more sensitive and undergo changes of more than 25% for a much smaller variation of the parameter $R$. Thus, the sensitivity obtained in the current approach is approximately 4–5 orders of magnitude higher than linear methods. The advantages of the proposed analysis are accompanied by a few limitations. The most important limitation is the requirement that a chaotic oscillation be present. However, this limitation may be overcome when a chaotic excitation may be provided to the system.

## Conclusions

The dynamics of an aeroelastic system composed of a panel forced by unsteady buffeting aerodynamic loads and undergoing limit-cycle oscillations and chaos has been investigated. The nonlinear von Kármán plate theory has been used to obtain a model for the panel, whereas a linear piston theory has been used to model the quasi-steady flow forcing the panel. The focus has been on detecting parametric changes in the system. The upstream endpoint of the panel has been considered supported by a spring of variable stiffness. Changes of 15% in the stiffness of the spring have been detected by exploring the chaotic dynamics of the panel. The sensitivity of the chaotic behavior to parametric changes has been shown to be an effective tool in detecting structural changes. A finite difference method has been used to simulate the dynamics of the aeroelastic system, and coherent structures of the panel dynamics have been identified using proper orthogonal decomposition. The sensitivity of the dynamics of the coherent structures to parametric changes has been discussed. The dynamics of the panel and flow have been decomposed along a basis of the vector space spanned by the dominant structures of the dynamics. Poincaré sections of the strange attractors for each coherent structure have been used to detect parametric changes.

The relative distributions of points in the Poincaré sections have been investigated to detect changes in their geometric appearance (by using histograms and first-order inertial moments of sets of points). A more quantitative measure of the change in the geometric characteristics of the attractors and the extent, level, and location of the damage is highly desirable, and future research will address it in detail. The current paper has addressed two other complementary issues, that is, the existence and importance of the coherent structures and the level of (high) sensitivity of the geometric shape of the attractor to parametric variations in the aeroelastic system.

## References

[1]Cusumano, J. P., and Chatterjee, A., "Steps Towards a Qualitative Dynamics of Damage Evolution," *International Journal of Solids and Structures*, Vol. 37, No. 44, 2000, pp. 6397–6417.

[2]Farrar, C. R., Doebling, S. W., and Nix, D. A., "Vibration-Based Structural Damage Identification," *Philosophical Transactions of the Royal Society of London, Series A: Mathematical, Physical and Engineering Sciences*, Vol. 359, No. 1778, 2001, pp. 131–149.

[3]Feeny, B. F., Yuan, C. M., and Cusumano, J. P., "Parametric Identification of an Experimental Magneto-Elastic Oscillator," *Journal of Sound and Vibration*, Vol. 247, No. 5, 2001, pp. 785–806.

[4]Chatterjee, A., Cusumano, J. P., and Chelidze, D., "Optimal Tracking of Parameter Drift in a Chaotic System: Experiment and Theory," *Journal of Sound and Vibration*, Vol. 250, No. 5, 2002, pp. 877–901.

[5]Chelidze, D., Cusumano, J. P., and Chatterjee, A., "A Dynamical Systems Approach to Damage Evolution Tracking, Part 1: Description and Experimental Application," *Journal of Vibration and Acoustics*, Vol. 124, No. 2, 2002, pp. 250–257.

[6]Cusumano, J. P., Chelidze, D., and Chatterjee, A., "A Dynamical Systems Approach to Damage Evolution Tracking, Part 2: Model-Based Validation and Physical Interpretation," *Journal of Vibration and Acoustics*, Vol. 124, No. 2, 2002, pp. 258–264.

[7]Agbabian, M. S., Masri, S. F., Miller, R. F., and Caughey, T. K., "System Identification Approach to Detection of Structural Changes," *Journal of Engineering Mechanics*, Vol. 117, No. 2, 1990, pp. 370–390.

[8]Ghanem, R., and Shinozuka, M., "Structural System Identification: Theory," *Journal of Engineering Mechanics*, Vol. 121, No. 2, 1995, pp. 255–264.

[9]Loh, C. H., and Tou, I. C., "A System Identification Approach to the Detection of Changes in both Linear and Nonlinear Structural Parameters," *Earthquake Engineering and Structural Dynamics*, Vol. 24, No. 1, 1995, pp. 85–97.

[10]Smyth, A. W., Masri, S. F., Caughey, T. K., and Hunter, N. F., "Surveillance of Mechanical Systems on the Basis of Vibration Signature Analysis," *Journal of Applied Mechanics*, Vol. 67, No. 3, 2000, pp. 540–551.

[11]Sohn, H., and Farrar, C. R., "Damage Diagnosis Using Time Series Analysis of Vibration Signals," *Smart Materials and Structures*, Vol. 10, No. 3, 2001, pp. 446–451.

[12]Pandey, A. K., and Biswas, M., "Damage Detection in Structures Using Changes in Flexibility," *Journal of Sound and Vibration*, Vol. 169, No. 1, 1994, pp. 3–17.

[13]Ljung, L., *System Identification—Theory for the User*, Prentice–Hall, New York, 1999.

[14]van Overschee, P., and DeMoor, B., *Subspace Identification for Linear Systems: Theory, Implementation and Applications*, Kluwer, New York, 1996.

[15]Shinozuka, M., and Ghanem, R., "Structural System Identification: Experimental Verification," *Journal of Engineering Mechanics*, Vol. 121, No. 2, 1995, pp. 265–273.

[16]Sato, T., and Qi, K., "Adaptive H-infinity Filter: Its Application to Structural Identification," *Journal of Engineering Mechanics*, Vol. 124, No. 11, 1998, pp. 1233–1240.

[17]Smyth, A. W., Masri, S. F., Chassiakos, A. G., and Caughey, T. K., "On-line Parametric Identification of MDOF Nonlinear Hysteretic Systems," *Journal of Engineering Mechanics*, Vol. 125, No. 2, 1999, pp. 133–142.

[18]Pecora, L. M., and Caroll, T. L., "Discontinuous and Nondifferentiable Functions and Dimension Increase Induced by Filtering Chaotic Data," *Chaos*, Vol. 6, No. 3, 1996, pp. 432–439.

[19]Trickey, S. T., Todd, M., Seaver, M., and Nichols, J., "Geometric Time Domain Methods of Vibration Based Damage Detection," *Proceedings of the SPIE 9th Smart Structures and Materials Conference*, Vol. 1, Society of Photo-Optical Instrumentation Engineers (International Society for Optical Engineering), Bellingham, WA, 2002, pp. 1–9.

[20]Banks, H. T., Joyner, M. L., Wincheski, B., and Winfree, W. P., "Nondestructive Evaluation Using a Reduced-Order Computational Methodology," *Inverse Problems*, Vol. 16, No. 4, 2000, pp. 929–945.

[21]Zimmerman, D. C., Smith, S. W., Kim, H. M., and Bartkowicz, T. J., "An Experimental Study of Structural Health Monitoring Using Incomplete Measurements," *Journal of Vibration and Acoustics*, Vol. 118, No. 4, 1996, pp. 543–550.

[22]Epureanu, B. I., and Dowell, E. H., "Reduced Order System Identification of Nonlinear Aeroelastic Systems," *Proceedings of the First M.I.T. Conference on Computational Fluid and Solid Mechanics*, Vol. 1, Elsevier, Boston, 2001, pp. 1152–1160.

[23]Epureanu, B. I., Hall, K. C., and Dowell, E. H., "Reduced Order Models of Unsteady Transonic Viscous Flows in Turbomachinery," *Journal of Fluids and Structures*, Vol. 14, No. 8, 2000, pp. 1215–1235.

[24]Epureanu, B. I., Hall, K. C., and Dowell, E. H., "Reduced Order Models of Unsteady Viscous Flows in Turbomachinery Using Viscous–Inviscid Coupling," *Journal of Fluids and Structures*, Vol. 15, No. 2, 2001, pp. 255–276.

[25]Holmes, P., Lumley, J. L., and Berkooz, G., *Turbulence, Coherent Structures, Dynamical Systems and Symmetry*, Univ. Press, Cambridge, MA, 1996.

[26]Sirovich, L., "Turbulence and the Dynamics of Coherent Structures, Part I: Coherent Structures," *Quarterly of Applied Mathematics*, Vol. 45, No. 3, 1987, pp. 561–571.

[27]Feeny, B. F., "On the Proper Orthogonal Modes and Normal Modes of Continuous Vibration Systems," *Journal of Vibration and Acoustics*, Vol. 124, No. 1, 2002, pp. 157–160.

[28]Kappagantu, R. V., and Feeny, B. F., "Part I: Dynamical Characterization of a Frictionally Exited Beam," *Nonlinear Dynamics*, Vol. 22, No. 4, 2000, pp. 317–334.

[29]Feeny, R. V. K. B. F., "Part II: Proper Orthogonal Modal Modeling of a Frictionally Excited Beam," *Nonlinear Dynamics*, Vol. 23, No. 1, 2000, pp. 1–11.

[30]Dowell, E. H., and Voss, H. M., "Theoretical and Experimental Panel Flutter Studies in the Mach Number Range 1.0 to 5.0," *AIAA Journal*, Vol. 3, No. 12, 1965, pp. 2292–2304.

[31]Dowell, E. H., "Nonlinear Oscillations of a Fluttering Plate," *AIAA Journal*, Vol. 4, No. 7, 1966, pp. 1267–1275.

[32]Dowell, E. H., "Nonlinear Oscillations of a Fluttering Plate. II," *AIAA Journal*, Vol. 5, No. 10, 1967, pp. 1856–1862.

[33]Dowell, E. H., and Ventres, C. S., "Comparison of Theory and Experiment for Nonlinear Flutter of Loaded Plates," *AIAA Journal*, Vol. 8, No. 9, 1970, pp. 2022–2030.

[34]Dowell, E. H., *Aeroelasticity of Plates and Shells*, Noordhoff International, Leyden, The Netherlands 1975, Chap. 3.

[35]Reynolds, R. R., "On the Nonlinear Aeroelasticity of Panels," Ph.D. Dissertation, Dept. of Mechanical Engineering and Materials Science, Duke Univ., Durham, NC, May 1993.

[36]Azeez, M. F. A., and Vakakis, A. F., "Proper Orthogonal Decomposition of a Class of Vibroimpact Oscillations," *Journal of Sound and Vibration*, Vol. 240, No. 5, 2000, pp. 859–889.

[37]Lighthill, M. J., "Oscillating Airfoils at High Mach Number," *Journal of the Aeronautical Sciences*, Vol. 20, No. 6, 1953, pp. 402–406.

[38]Dowell, E. H., *A Modern Course in Aeroelasticity*, 2nd ed., Kluwer Academic, Dordrecht, The Netherlands, 1989, Chaps. 1 and 2.

[39]Dowell, E. H., "Flutter of a Buckled Plate as an Example of Chaotic Motion of a Deterministic Autonomous System," *Journal of Sound and Vibration*, Vol. 85, No. 3, 1982, pp. 333–344.

[40]Kim, D. H., and Lee, I., "Transonic and Low-Supersonic Aeroelastic Analysis of a Two-Degree-of-Freedom Airfoil With a Freeplay Non-Linearity," *Journal of Sound and Vibration*, Vol. 234, No. 5, 2000, pp. 859–880.

[41]Silva, W. A., "Reduced-Order Models Based on Linear and Nonlinear Aerodynamic Impulse Responses," *Proceedings of the CEAS/AIAA/ICASE/NASA Langley International Forum on Aeroelasticity and Structural Dynamics*, AIAA, Reston, VA, 1999, pp. 1731–1738.

[42]Bolotin, V. V., Grishko, A. A., Kounadis, A. N., and Gantes, C. J., "The Fluttering Panel as a Continuous Nonlinear Nonconservative System," *Journal of Vibration and Control*, Vol. 7, No. 2, 2001, pp. 233–247.

[43]Bolotin, V. V., Grishko, A. A., Kounadis, A. N., and Gantes, C. J., "Non-linear Panel Flutter in Remote Post-Critical Domains," *International Journal of Non-linear Mechanics*, Vol. 33, No. 5, 1998, pp. 753–764.

[44]Bolotin, V. V., Grishko, A. A., Kounadis, A. N., and Gantes, C. J., "Influence of Initial Conditions on the Postcritical Behavior of a Nonlinear Aeroelastic System," *Nonlinear Dynamics*, Vol. 15, No. 1, 1998, pp. 63–81.

[45]Epureanu, B. I., Tang, L. S., and Paidoussis, M. P., "Coherent Structures and Their Influence on the Dynamics of Aeroelastic Panels," *International Journal of Non-Linear Mechanics*, Vol. 39, No. 6, 2004, pp. 977–991.

[46]Epureanu, B. I., Tang, L. S., and Paidoussis, M. P., "Observations of the Dynamics of Panels in Supersonic Flow," *Proceedings of the Second M.I.T. Conference on Computational Fluid and Solid Mechanics*, Vol. 2, Elsevier, Boston, 2003, pp. 1332–1336.

[47]Niho, T., Horie, T., and Tanaka, Y., "Numerical Instability of Magnetic Damping Problem of Elastic Plate," *IEEE Transactions on Magnetics*, Vol. 36, No. 4, Pt. 1, 2000, pp. 1374–1377.

[48]Reynolds, R. R., Virgin, L. N., and Dowell, E. H., "High-Dimensional Chaos Can Lead to Weak Turbulence," *Nonlinear Dynamics*, Vol. 4, No. 1, 1993, pp. 531–546.

[49]Reynolds, R. R., and Dowell, E. H., "Nonlinear Aeroelastic Response of Panels," *Proceedings of 34th AIAA/ASME/ASCE/ASC Structures, Structural Dynamics, and Materials Conference*, Vol. 1, AIAA, Washington, DC, 1993, pp. 1–13.

[50]Jang, M. J., and Chen, C. K., "Bifurcation Analysis in Flexible Rotor Supported by Active Magnetic Bearing," *International Journal of Bifurcation and Chaos*, Vol. 11, No. 8, 2001, pp. 2163–2178.

[51]Paidoussis, M. P., *Fluid-Structure Interactions: Slender Structures and Axial Flow*, Academic Press, San Diego, CA, 1998, Chap. 5.

[52]Paidoussis, M. P., and Botez, R. M., "Chaotic Dynamics of Articulated Cylinders in Confines Axial Flow," *Journal of Fluids and Structures*, Vol. 7, 1993, pp. 719–750.

[53]Paidoussis, M. P., "Stability of a Chain of Cylinders Travelling Underwater," *Proceedings of 5-th International Offshore Mechanics and Arctic Engineering Symposium*, Vol. 1, American Society of Mechanical Engineers, Fairfield, NJ, 1986, pp. 483–490.

[54]Copeland, G. S., and Moon, F. C., "Chaotic Flow-Induced Vibration of a Flexible Tube with End Mass," *Journal of Fluids and Structures*, Vol. 6, No. 3, 1992, pp. 705–718.

[55]Langthjem, M. A., and Sugiyama, Y., "Dynamic Stability of Columns Subjected to Follower Loads: A Survey," *Journal of Sound and Vibration*, Vol. 238, No. 5, 2000, pp. 809–851.

[56]Thothandri, M., and Moon, F. C., "An Investigation of Nonlinear Models for a Cylinder Row in a Cross Flow," *Journal of Pressure Vessel Technology*, Vol. 121, No. 1, 1999, pp. 133–141.

[57]Turner, K. L., Miller, S. A., Hartwell, P. G., MacDonald, N. C., Strogatz, S. H., and Adams, S. G., "Five Parametric Resonances in a Microelectromechanical System," *Nature*, Vol. 396, No. 6707, 1998, pp. 149–152.

[58]Miller, S. A., Turner, K. L., and MacDonald, N. C., "Microelectromechanical Scanning Probe Instruments for Array Architectures," *Review of Scientific Instruments*, Vol. 68, No. 11, 1997, pp. 4155–4162.

[59]Abarbanel, H. D. I., *Analysis of Observed Chaotic Data*, Springer-Verlag, Berlin, 1996.

[60]Abarbanel, H. D. I., Brown, R., Sidorowich, J. J., and Tsimring, L. S., "The Analysis of Observed Chaotic Data in Physical Systems," *Reviews of Modern Physics*, Vol. 65, No. 4, 1993, pp. 1331–1392.

[61]Kantz, H., and Schreiber, T., *Nonlinear Time Series Analysis*, Cambridge Univ. Press, New York, 1997.

[62]Moon, F. C., *Chaotic and Fractal Dynamics: An Introduction for Applied Scientists and Engineers*, Wiley, New York, 1992, Chap. 7.

[63]Parker, T. S., and Chua, L. O., *Practical Numerical Algorithms for Chaotic Systems*, Springer-Verlag, New York, 1989.

[64]Bow, T. S., *Pattern Recognition and Image Preprocessing*, Marcel Dekker, New York, 2002.

[65]Pavlidis, T., *Algorithms for Graphics and Image Processing*, Computer Science, Rockville, MD, 1982.

E. Livne
*Associate Editor*